

Low-energy-electron stimulated desorption of metastable particles from condensed N₂ and CO

H. Shi, P. Cloutier, and L. Sanche

*Groupe du Conseil de Recherches Medicales en Science des Radiations, Faculté de Médecine,
Université de Sherbrooke, Sherbrooke, Quebec, Canada J1H 5N4*

(Received 27 March 1995)

The impact of low-energy electrons (7–19 eV, $\Delta E = 60$ meV) is found to induce desorption of metastable particles (N₂^{*} and CO^{*}) from condensed multilayer N₂ and CO films. For N₂ films, the yield function of the metastable-particle signal, which shows two regions (below and above 11 eV) of large intensity difference, is assigned to excitations to the valence state $B^3\Pi_g$ and to the Rydberg state $E^3\Sigma_g^+$, respectively. Desorption of N₂^{*} above 11 eV is believed to be due to the repulsive interaction between the excited molecules and the solid surface. The desorption yield of CO^{*}, which is much weaker than that for N₂^{*}, is discussed in terms of vibrational energy transfer from the vibrational excited $a'^3\Sigma^+$ state.

I. INTRODUCTION

Electron impact on surfaces leads to a mixture of events, including the desorption of positive and negative ions as well as neutral species in ground and excited states. These events show the diversity of relaxation processes following electronic excitation. Desorption of species in long-lived electronically excited states (i.e., metastable species) has been observed in electronically stimulated desorption from condensed rare-gas solids,^{1–6} as well as from chemisorbed layers on metals.^{7–10} To our knowledge, there exists no report on the desorption of metastable particles from a molecular solid. However, desorption of ground-state neutrals from molecular solids like N₂ and CO has been investigated by excitation with high-energy electrons, photons, or fast light ions.^{11–15} A microscopic model has been derived from yield data of condensed N₂ and O₂.¹¹ The first step is assumed to be the primary excitation of singly charged positive molecular ions, which then dissociate upon neutralization. From the same model, it has been suggested¹¹ that the total amount of energy transferred to the dissociation fragments by the electronic decay reactions is 3 eV in the case of N₂. These fragments would desorb neighboring molecules via collision cascade when the decay occurs near the surface. However, the kinetic-energy distributions for N₂ and N desorbed from solid N₂ (Refs. 14 and 15) indicate that the kinetic energy of the fragment N reaches 6 eV. Furthermore, the amount of the fast particles is smaller than expected from the above model with the maximum of translational energy lying between 30 and 200 meV.¹⁵ It has been concluded^{14,15} that other electronic relaxation processes have to be considered in order to obtain a more complete understanding of the microscopic nature of the desorption phenomenon.

Here we report results of metastable-particle (MP) desorption from molecular solids. MP desorption is induced by a monochromatic electron beam impinging at low energy on condensed N₂ and CO multilayer films. N₂ and CO are isoelectronic and have many similar physical properties as shown in Table I.^{12,16} A comparison of

their electron-stimulated desorption (ESD) behavior is therefore expected to be revealing.

II. EXPERIMENT

The experiment was performed in an ultrahigh-vacuum system reaching a base pressure of $\sim 10^{-10}$ Torr. The apparatus has been described in detail previously.⁵ Briefly, a well-collimated low-energy (1–20 eV) electron beam impinges on a Pt(111) single crystal at 18° with respect to the surface normal; the desorbed metastable particles are measured with a large area microchannel plate (MCP) array which is superimposed on a position-sensitive anode. The electron beam has an intensity of 5 nA and an energy resolution of 60-meV full width at half maximum. In the present experiment, the electron energy is swept between 5 and 19 eV with respect to the vacuum level. As explained in Sec. III, this range limits the detected metastable species to molecular excited states (i.e., N₂^{*} and CO^{*}). The energy of the vacuum level is calibrated within ± 0.3 eV by measuring the onset of the target current as the voltage applied between the electron source and the target is slowly increased. The crystal, which is mounted on the tip of a closed-cycle helium cryostat, can be cooled to 20 K and cleaned by electrical heating and Ar bombardment. The target films are grown on the Pt(111) surface by condensing from the vapor phase N₂ and CO gases. The latter were supplied by Matheson of Canada Ltd. with a purity of 99.9995% and 99.99%, respectively.

TABLE I. Molecular properties of CO and N₂. n , molecular number density; R , equilibrium separation of atoms in the molecules; I , ionization potential; D_0 , dissociation energy; $h\nu$, vibrational energy spacing in ground state; and U_s , sublimation energy. Properties are gas phase except for n and U_s (from Refs. 12 and 16).

Molecule	n (\AA^{-3})	R (\AA)	I (eV)	D_0 (eV)	$h\nu$	U_s (eV)
N ₂	2.2×10^{-2}	1.09	15.6	9.8	0.29	0.075
CO	2.2×10^{-2}	1.13	14.0	11.1	0.27	0.088

The thickness of a film is estimated from the amount of gas introduced and the quantity required to build the first layer. The latter is inferred from temperature programmed desorption.⁵

Metastable species reaching the surface of a MCP detector transfer their excitation energies via an Auger-type process causing secondary-electron ejection. In the present detector the threshold energy for the detection of metastable particles is estimated to lie around 6 eV.⁵ We use a pile of three standard MCP's (Galileo) with an Inconel metallic coating facing the sample. According to the manufacturer, the UV detection efficiency without a high-yield photocathode coating lies around 5–10% for photon energies above 10 eV and drops by about three orders magnitude for 8-eV photons. The low secondary-electron emission coefficient for photons is due to their weak interaction with the bulk of the MCP material, which results in a relatively large penetration depth. On the average, secondary electrons will be excited far away from the MCP surface and only a small fraction of them will be able to leave the bulk and start an electron avalanche. Owing to the much lower detection efficiency for UV compared to that of metastable particles, we consider the measured signals to arise essentially from desorbed metastable particles. This assumption is verified by the time-of-flight (TOF) measurements which show a near-zero magnitude from prompt photons. TOF measurements are performed by switching on the electron beam for a short period (10 μ s) and subsequently recording the arrival time of those particles which trigger the MCP's. The accuracy of the TOF measurement is limited by the duration of the electron pulse (i.e., $\Delta t = \pm 5 \mu$ s). The path length (d) between the target and the MCP is 5.2 ± 0.1 cm. This parameter is related to the kinetic energy $E(t)$ of the metastable particles by the relation

$$E(t) = \frac{M}{2} \left(\frac{d}{t} \right)^2, \quad (1)$$

where M is the mass of the metastable particle (28 amu for N_2 and CO), and t is the time of flight. From this relation, we find

$$\Delta E(t) = \frac{Md}{t^2} \left[\Delta d + \frac{d}{t} \Delta t \right] \quad (2)$$

for the resolution in translational energy of the metastable particles.

III. RESULTS

The MP desorption yield function obtained for a N_2 film having a thickness of 50 ML is shown in Fig. 1. The distribution can be divided in two parts: one has a threshold of about 7.2 eV and reaches a plateau at 9.0 eV; the other has a threshold near 11.5 eV and rises sharply with increasing electron energy up to 14.5 eV. At higher electron energies, the desorption yield increases further with a smaller slope up to 50 eV (not shown).

The MP signal is interpreted as due to N_2^* . Considering the possibility of N^* production, any such species would involve dissociation of a N_2^* state having an energy

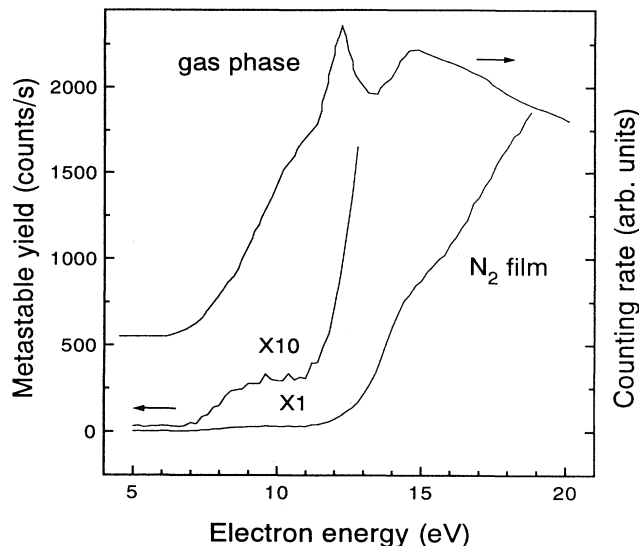


FIG. 1. Yield function of metastable-particle desorption from a 50-ML N_2 film and production from gaseous N_2 (Ref. 18). The yield in the threshold region is enlarged by a factor of 10 ($\times 10$).

higher than at least 16 eV since the lowest dissociation limit is close to 10 eV (Ref. 16) (see also Table I) and the internal energy of a fragment must be about 6 eV to be detected. This excludes atomic nitrogen (N^*) as being the metastable species responsible for the 7.2- and 11.5-eV thresholds and the broad maximum at 14.5 eV.

Experimental results have been reported on yield functions for metastable states of N_2 and CO in the gas phase.^{17,18} The yield function for the production of metastable nitrogen reported by Borst and Zipf¹⁸ is shown in Fig. 1 for comparison. It exhibits a threshold at about 7 eV. For N_2 metastable excitation in the gas phase,^{17,18} the $B^3\Pi_g$ state is excited with a much higher relative intensity than the $A^3\Sigma_u^+$ state in the threshold region. Electronic transitions from the nitrogen-molecule ground state to the lower vibrational levels of the $A^3\Sigma_u^+$ state are not possible, owing to the difference in equilibrium internuclear separation of these states.¹⁶ The $a^1\Pi_g$ state also appears to have a low relative intensity in the threshold region.¹⁷ A narrow peak in the metastable yield at about 12 eV has been assigned to excitation of the $E^3\Sigma_g^+$ state. The broader peak at about 15 eV is due mainly to contributions from the $a^1\Pi_g$ state.^{17,18} The MP desorption threshold of 7.2 eV for the N_2 film lies near the threshold for excitation of the $B^3\Pi_g$ state of N_2 , while the energy of 11.5 eV corresponds to the excitation threshold of the $E^3\Sigma_g^+$ state.¹⁶

TOF distributions for N_2^* from a 50-ML N_2 film bombarded with 8.5-, 13.5-, and 27.0-eV electrons are shown in Fig. 2. For an incident energy of 13.5 and 27.0 eV, the TOF distributions look similar to each other. With 8.5-eV electrons, the MP signal peaks around a kinetic energy of 70 ± 12 meV. For 13.5- and 27.0-eV incident electrons, a fast component is superimposed on this lower kinetic-energy distribution. It results in a MP desorption

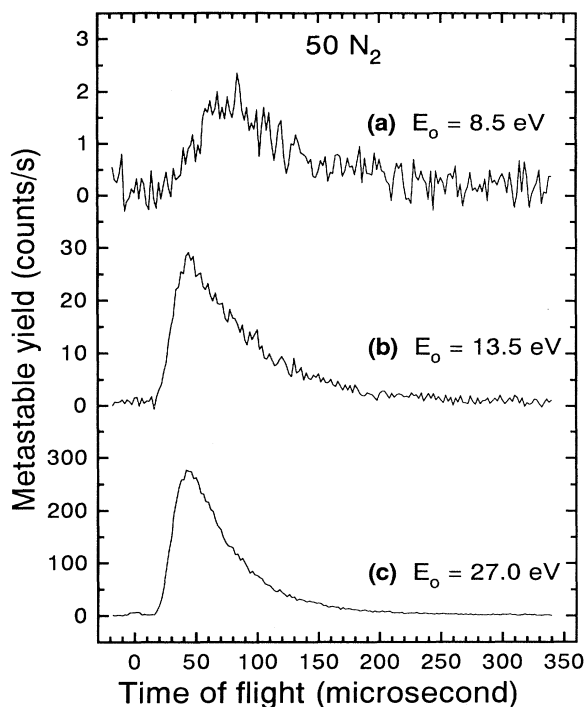


FIG. 2. Time-of-flight distributions of metastable particles desorbed from a 50-ML N_2 film by the impact of electrons of (a) 8.5 eV, (b) 13.5 eV, and (c) 27.0 eV.

yield having a TOF peak located at a kinetic energy of 204 ± 54 meV. These TOF distributions are incompatible with the expected distribution from N^* states arising from dissociating N_2^* states (i.e., $N_2^* \rightarrow N + N^*$). Such atomic metastable particles should be produced with eV's of energy thus forming TOF distributions which, according to Eq. (1), would peak around $8 \mu s$ (i.e., near the origin).

The yield function for MP desorption from a 50-ML CO film is shown in Fig. 3. The signal is approximately an order of magnitude weaker than that for N_2 films. The threshold of the MP desorption lies around 8.0 eV, and the yield increases continuously with electron energy. A broad peak is observed at about 15 eV. As in the case of N_2 , interpretation of the signal as due to metastable CO^* is dictated by the elimination of the other possibilities. The metastable yield function for CO in the gas phase, taken from Ref. 18, is shown at the top of Fig. 3. It exhibits an onset at 6 eV due to excitation of the $a^3\Pi$ state. The higher-lying state $b^3\Sigma^+$ is considered to contribute to the signal at electron energies above 10.5 eV.^{17,18} The MP desorption threshold of 8.0 eV for the CO film is higher than that in the gas phase.

The TOF distributions for CO^* from 50-ML CO bombarded with 11.0-, 15.0-, and 23.0-eV electrons (not shown) are very similar to each other in shape and energy. They exhibit a single TOF peak whose position corresponds to a kinetic energy of 195 ± 51 meV. As in the case of the N_2 TOF distributions, the photon signal at $t=0$ is barely perceivable.

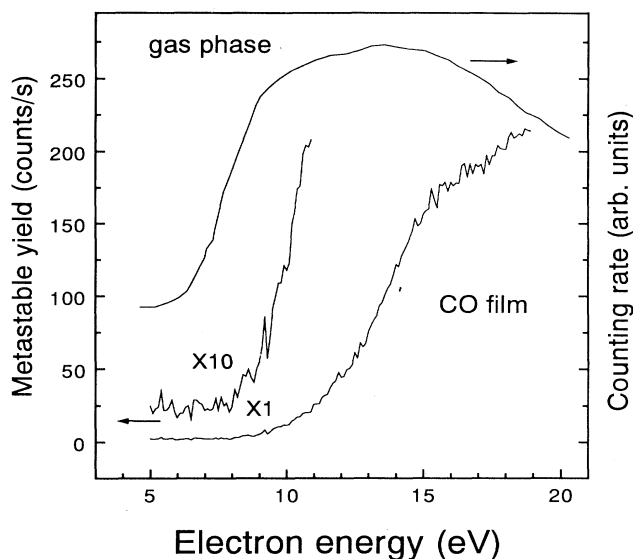


FIG. 3. Yield function of metastable-particle desorption from a 50-ML CO film and production from gas-phase CO (Ref. 18).

IV. DISCUSSION

In recent high-resolution-electron-energy-loss (HREEL) experiments, it has been found that the energies and amplitudes of the valence electronically excited states of multilayer N_2 and CO films are only slightly changed from their gas-phase analogs.¹⁹ The energy levels of the observed valence states are shifted down by a few tens of meV with respect to the gas-phase values, while Rydberg states fuse into a broad continuum. Above the energy for excitation of Rydberg states, only the valence state manifold bears a resemblance to the gas-phase spectra. In fact, below this threshold, we can assume that in the bulk and near the film surface, the same states as in the gas phase are excited with essentially the same magnitude and energy. The yield function of metastable states in the gas phase can therefore be of considerable help in understanding the desorption of metastable particles from a condensed film. Below the Rydberg state energies, large differences between the gas- and condensed-phase data are expected to result from modifications of the yield by the desorption mechanism operative at the film surface. In other words, only those metastable particles that desorb can be measured in our experiment. The difference in the metastable yield between the condensed films and the gas phase is therefore directly related to the desorption probability and mechanism. We first discuss the assignment of the states producing the MP signal and then explain the possible desorption mechanisms.

Some profound differences are observed in the yield functions between condensed- and gas-phase N_2 . However, since the same states are excited electronically with essentially the same magnitude in both phases, we assign the signal threshold of 7.2 eV and that between impact energies of 7 and 11 eV in Fig. 1 as due to excitation of

the $B^3\Pi_g$ state, in compliance with the gas-phase interpretation.^{17,18} The TOF distribution for an impact energy of 8.5 eV in Fig. 2(a) is therefore assigned to a MP signal induced by excitation of the $B^3\Pi_g$ state. The lifetime of that state is 4–8 μs ,¹⁶ but the detected signal in Fig. 2(a) has an average flight time of 75 μs . Desorbed N_2 molecules in the $B^3\Pi_g$ state are therefore expected to decay to a lower state during their TOF. We conclude that the detected species are in the $A^3\Sigma_u^+$ state.

For the energy region above 11 eV, we observed a sharp increase in MP signal starting at about 11.5 eV. This energy agrees well with the excitation threshold for the first Rydberg state $E^3\Sigma_g^+$. Thus we tend to assign the MP signal in this region to excitation of this state. The lifetime of the $E^3\Sigma_g^+$ state is 190 μs ;¹⁸ i.e., sufficiently long to be detected in our experimental arrangement. The $E^3\Sigma_g^+$ and $a''^1\Sigma_g^+$ states (11.87 and 12.25 eV) are the two lowest triplet-singlet Rydberg states derived from the $X^2\Sigma_g^+$ ion core of N_2 . The $E^3\Sigma_g^+$ state is the upper state of the $E^3\Sigma_g^+-A^3\Sigma_u^+$ Herman-Kaplan system and the $a''^1\Sigma_g^+$ state is the upper state of the $a''^1\Sigma_g^+-X^1\Sigma_g^+$ Dressler-Lutz system.¹⁶ The cross sections for low-energy electron-impact excitation of the a'' state is about one order of magnitude larger than that for the E state.²⁰ However, the lifetime of the a'' state has been accurately measured to be $3.49 \pm 0.10 \mu\text{s}$,²¹ and its main decay mode is believed to be predissociation rather than emission of radiation.²¹ This lifetime is much smaller than our TOF resolution. Desorbed N_2 in the a'' state (if any) should decay to atomic N ($4S^0+4S^0$ or $4S^0+2D^0$) in their TOF, which is not expected to contribute to the MP signal.

In the gas phase, the excitation of the $E^3\Sigma_g^+$ state is enhanced by the decay of a core-excited shape resonance near 12 eV into its parent, the E state,²² producing a narrow peak in its excitation function. This resonance seems absent in N_2 films, but a broad peak appears at 14.5 eV where a peak is also found in the gas-phase yield function. The peak, at about 15 eV in the gas phase, arises from excitation of the configuration $a^1\Pi_g$. As seen in Fig. 1, the contribution from this state is much weaker in the N_2 film. Being a valence state, the MP signal from the $a^1\Pi_g$ state is expected to be of similar magnitude as that from the $B^3\Pi_g$ state. From Fig. 1 its contribution to desorption is estimated at its maximum to be about 15% of the Rydberg state signal, which is about three times the magnitude of the MP signal of the $B^3\Pi_g$ state.

The MP desorption threshold for CO films is observed at 8.0 eV (Fig. 3), while for metastable production in the gas phase the excitation threshold lies at 6.0 eV and is due to the excitation of the $a^3\Pi$ state. Below 10 eV, HREEL spectra¹⁹ are similar for gas and solid, so we must conclude that although considerable excitation to the $a^3\Pi$ state also occur in a CO film it does not desorb. The threshold energy of 8.0 eV can be related to the excitation threshold of the $A^1\Pi$ state,¹⁶ but this state undergoes an allowed transition to the ground state with a radiative lifetime of about 9 ns,²³ and therefore should not contribute to the MP signal. According to HREEL spectra,¹⁹ the only other state which is produced with a non-negligible amplitude by 8–10-eV electrons in solid CO

has the configuration $a'^3\Sigma^+$. We therefore believe it is this state that contributes to the MP signal from a CO film in the range 8–10 eV.

At low electron-impact energies, the desorption process must be simple since ionization, desorption of dissociation fragments, and desorption via collision cascade can be excluded. There are only two possibilities for the desorption of excited molecules from a molecular solid. In one case, the excited molecule at the surface has an energy higher than in the gas phase. Motion along a repulsive molecule-surface potential-energy curve can lead to acceleration and desorption of the excited molecule. Such an energy balance has been found to allow desorption of Ar^* from Ar films and Xe^* from Xe/Kr films (i.e., Xe adsorbed on a Kr multilayer film), but not the desorption of Kr^* from Kr films and Xe^* from Xe films.⁶ The so-called cavity expulsion mechanism can be included in this scheme. This mechanism was introduced for Ar crystals.¹ The excited atom or molecule located at the surface experiences a repulsive interaction with all neighbors if the matrix has a negative electron affinity, and this repulsive potential propels the excited species into vacuum. Inside the bulk, this repulsion would lead to a cavity around the excited particle. In crystals with a positive electron affinity, the excited particle is not expelled owing to the attractive interaction of the excited-orbit electron cloud with the neighboring atoms. Quantitative calculations²⁴ were able to predict details of the Ar^* desorption⁵ and the absence of cavity expulsion of Kr^* from Kr crystals. However, the desorption of Xe^* from the Xe/Kr film observed by Mann, Leclerc, and Sanche⁶ cannot be explained by cavity expulsion, since the electron affinity is positive. Local repulsive Xe^* -Kr interaction near the film surface must be considered to account for the ejection of Xe^* atom since, in this simple system, no other energy is available for desorption.

For vibrationally and electronically excited adsorbates having a lower energy than in the gas phase, another option is available for desorption: energy transfer from intramolecular vibrations to the molecule-surface bond followed by desorption of the molecule in lower vibrational levels of the excited state. Experimental and theoretical evidence has been given in the literature for this process.^{25–31} Photon-stimulated desorption due to internal vibrational excitation of adsorbed molecules has been demonstrated by Heidberg, Stein, and Riehl²⁵ for the system CH_3F on NaCl, by Chuang²⁶ for pyridine on KCl and silver, and by Chuang and co-workers²⁷ for NH_3 and ND_3 on Cu(100), NaCl, and Ag films. Generally, for physisorbed systems, the energy of the internal vibrational mode of the adsorbed molecules $\hbar\Omega$ is much larger than the spacing between the energies ($E_{i+1}-E_i$) of bound states (i) in the surface potential; i.e., the internal vibrational frequency of the molecule is larger than the molecule-surface (i.e., external) oscillation vibrational frequency. In the harmonic-oscillator approximation, the energy of the internal vibrational modes of the adsorbed molecules is given by $E_i^v = E_i + (v + \frac{1}{2})\hbar\Omega$, where v is the excited internal quantum. If the adsorbed molecule is excited into a vibrational state such that its total vibrational

energy $E_i^v = E_i + (v + \frac{1}{2})\hbar\Omega = (P^2/2m) + (v' + \frac{1}{2})\hbar\Omega$ is degenerate with the continuum state of momentum P , then elastic tunneling into the latter state²⁸ or inelastic tunneling (i.e., aided by the emission and adsorption of phonons²⁹ and/or molecule-surface librational energy³⁰) will lead to desorption of the molecule in a lower vibrational level (v'). However, such a transfer of vibrational energy must take place over times of the order of 10^{-9} – 10^{-11} s,²⁹ and would be ineffective if the excited-state lifetime is much shorter.

N_2 and CO are similar in various physical properties as shown in Table I. Some known energy levels for excitations in the bulk and in the gas phase are shown in Fig. 4; for N_2 and CO, the energies at the surface are taken to be intermediate between the gas- and condensed-phase values, as expected from HREEL measurements of surface excitons;³² those for the Xe/Kr system are taken from the results of Mann, Leclerc, and Sanche.⁶ In such a relatively simple atomic system, desorption is possible only when the energy at the surface is higher than that in the gas phase. The excitation energy for Xe* at the Kr surface must therefore be higher than that of the free Xe* (3P_2 8.31 eV) as shown in Fig. 4 since desorption of Xe* in vacuum is observed.⁶

The bulk $N_2(E)$ state in Fig. 4 is given a large energy width because of the broad continuum observed for Rydberg states in HREEL spectroscopy. N_2 has a negative electron affinity with the energy level of the bottom of the conduction band with respect to the vacuum level (V_0) at 0.8 eV, and CO has a positive electron affinity with $V_0 = -0.5$ eV.³³ This means that the cavity expulsion mechanism should be effective for N_2 but not for CO. It is therefore reasonable to assume that at the surface the Rydberg excited states of N_2 lie above the vacuum level, while all states for CO lie below. However, the energy of the valence states of N_2 have been measured precisely by

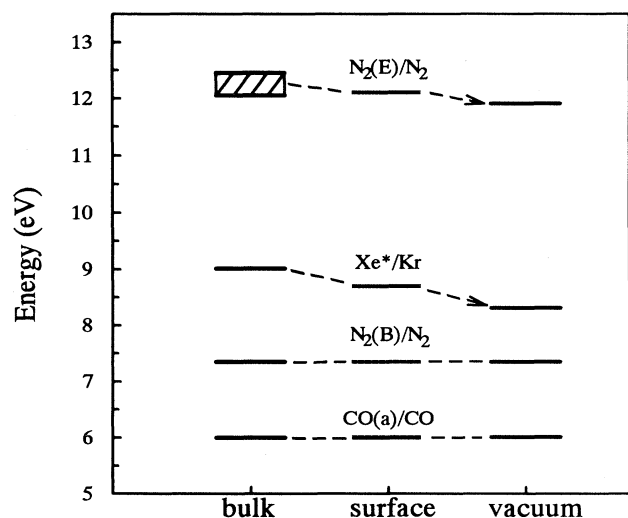


FIG. 4. Energy values for excitation of the state $a^3\Pi$ of CO, $B^3\Pi_g$ and $E^3\Sigma_g^+$ of N_2 , and the lowest electronically excited state of Xe in the gas phase, at the surface and in the bulk. The Xe*/Kr levels represent a Xe-doped Kr matrix.

HREELS (Ref. 19) to lie slightly below the vacuum level. Rydberg states have a larger radius than valence states, so that the larger repulsive forces between N_2^* and their neighbors place them at higher energies than those in valence orbital configurations. As observed in Figs. 1 and 2, this is consistent with a much stronger MP signal above 11 eV and metastable species of greater velocity, respectively. We therefore attribute N_2^* desorption above 11 eV to cavity expulsion. Excitation of $N_2(E)$ in the gas phase shows that essentially only $v=0$ is excited.^{17,18} This excludes the possibility of desorption via vibrational energy transfer. N_2^* desorption below 11 eV [i.e., desorption from the $N_2(B)$ state] will be addressed below.

The energy values for the CO(a) state in Fig. 4 is such that its desorption is energetically forbidden, in accordance with the experimental finding. According to the cavity expulsion mechanism the other CO states behave similarly so that no desorption should occur at all. A vibrational energy-transfer mechanism must therefore be involved to account for CO* desorption. Recent calculations by Dzegilenko, Herbst, and Uzer and Galloway and Herbst³⁰ shows that desorption of ground-state CO physisorbed on nonpolar substrates is highly dependent on the initial vibrational and librational populations. According to these results, for initial values of the stretching vibration quantum number lying within the range $v=0$ – 4 , desorption does not take place at all at short times ($t < 22.5$ ps) unless there is also significant librational excitation. On the other hand, if high values of these vibrational quanta are considered, desorption occurs on a picosecond time scale, even when the system is characterized by low phonon frequencies. In our experiment, the vibrational population of the CO molecules at the surface are determined by the Franck-Condon factors for the electronic transitions producing the metastable CO states. Using potential-energy diagram of CO and known molecular constants,¹⁶ a simple estimate gives a considerable magnitude for excitation of only the $v=0$ – 4 levels of the CO $a^3\Pi$ state (total internal excitation energy 6–7 eV) as observed experimentally by HREELS.¹⁹ It can be concluded that the vibrational excitation frequencies and energies in the $a^3\Pi$ state are too low to allow sufficient energy transfer to the molecule-surface bond during the lifetime of the surface $a^3\Pi$ state. Vibrational levels of $v=7$ – 24 for the CO $a'^3\Sigma^+$ state, however, are estimated to lie within the Franck-Condon region, and a threshold energy of 8 eV would correspond to $v=8$ for the $a'^3\Sigma^+$ state. It has been assumed by Mann *et al.*³⁴ that the $a'^3\Sigma^+$ and $d^3\Delta$ states of CO are formed by the energy transfer from the Xe exciton by excitation of a Xe film covered with CO, like the gas-phase reaction between Xe* and CO. The TOF data for CO* in Ref. 34 looks very similar to that for a pure CO film in this work. This is consistent with the assignment of the $a'^3\Sigma^+$ state as the metastable configuration responsible for the MP signal. The $a'^3\Sigma^+$ state has a lifetime of 4–10 μ s,³⁵ which is sufficiently long for vibrational energy transfer. This state is expected to decay to the $a^3\Pi$ configuration during the TOF.

Coming back to N_2^* desorption in the B state, we suggest that it is also induced by vibrational energy transfer.

The observed threshold would mean that, unlike the case of CO, low vibrational levels ($v=1-4$) in the $N_2(B)$ state could induce desorption. Energetically, this is possible since in condensed N_2 the electronic states between 6 and 11 eV lie less than 35 meV lower than the corresponding ones in vacuum. Within this energy range, MP desorption can also occur from higher vibrational levels of the $A^3\Sigma_u^+$ state following the decay of the $N_2(B)$ state at the surface. However, at higher electron-impact energies, dissociation of N_2 may occur causing a reduction in $N_2(A)$ desorption due to a coupling of the A triplet state with N atoms, as observed by Oehler, Smith, and Dressler;³⁶ e.g., $N_2(A, v') + N(^4S) \rightarrow N_2(X, v'') + N(^2D)$. With the present system, we cannot distinguish between N_2^* desorption in the A or B state.

V. CONCLUSION

We have shown that the use of monochromatic low-energy incident electrons can limit the number of induced events and therefore help to specify the orbital configuration of desorbing metastable molecules. By continuously varying the incident energy, we have also shown, that while Rydberg state excitation leads to a stronger desorption due to a repulsive interaction between the surface and the metastable particle, emission from the valence state is also possible by energy transfer

from the intramolecular vibrations to molecule-surface vibrational motion. Comparing the intensity of the MP signal of N_2 films to that of CO films, it appears that the cavity expulsion mechanism is more efficient than vibrational energy transfer for the desorption of metastable species from the surface of diatomic molecular solids. A more precise estimate of the contribution of each mechanism would have to include calculation of the metastable state lifetime at the surface and the magnitude of energy-transfer processes reducing the initial vibrational and librational populations of electronically excited states. Vibronic energy can be deexcited in $\Delta v=2$ steps by the exchange interaction with a ground-state molecule at a neighboring site,³⁷ e.g., $AB^*(v) + AB(v') \rightarrow AB^*(v-2) + AB(v'+2)$, thus reducing the vibrational energy of the metastable (AB^*) state and consequently desorption. Possible quenching of excited states by dissociation products, such as the strong coupling of $N_2(A)$ with $N(^4S)$ in the nitrogen matrix,³⁶ should also be taken into account in a more complete description of the desorption phenomenon.

ACKNOWLEDGMENTS

This work was sponsored by the Medical Research Council of Canada. We are indebted to Marc Michaud for helpful comments and fruitful discussions.

- ¹F. Coletti, J. M. Debever, and G. Zimmerer, *J. Phys. (Paris) Lett.* **45**, 467 (1984).
- ²T. Kloiber, W. Laasch, G. Zimmerer, F. Coletti, and J. M. Debever, *Europhys. Lett.* **7**, 77 (1988); T. Kloiber and G. Zimmerer, *Radiat. Eff. Defects Solids* **109**, 219 (1989); T. Kloiber and G. Zimmerer, *Phys. Scr.* **41**, 962 (1990).
- ³D. J. O'Shaughnessy, J. W. Boring, S. Cui, and R. E. Johnson, *Phys. Rev. Lett.* **61**, 1535 (1988); I. Arakawa, M. Takahashi, and K. Takeuchi, *J. Vac. Sci. Technol. A* **7**, 2090 (1989); I. Arakawa and M. Sakurai, in *Desorption Induced by Electronic Transitions, DIET IV*, edited by G. Betz and P. Varga (Springer, Berlin, 1990), p. 246; D. E. Weibel, A. Hoshino, T. Hirayama, M. Sakurai, and I. Arakawa, in *Desorption Induced by Electronic Transitions, DIET V*, edited by A. R. Burns, E. B. Stechel, and D. R. Jennison (Springer, Berlin, 1993), p. 333.
- ⁴G. Leclerc, A. D. Bass, M. Michaud, and L. Sanche, *J. Electron Spectrosc. Relat. Phenom.* **52**, 725 (1990).
- ⁵G. Leclerc, A. D. Bass, A. Mann, and L. Sanche, *Phys. Rev. B* **46**, 4865 (1992).
- ⁶A. Mann, G. Leclerc, and L. Sanche, *Phys. Rev. B* **46**, 9683 (1992).
- ⁷M. Kiskinova, A. Szabó, A.-M. Lanzillotto, and J. T. Yates, Jr., *Surf. Sci.* **202**, L559 (1988); M. Kiskinova, A. Szabó, and J. T. Yates, Jr., *ibid.* **202**, 215 (1988); R. D. Ramsier and J. T. Yates, Jr., *Surf. Sci. Rep.* **12**, 243 (1991); A. Szabó and J. T. Yates, Jr., in *Desorption Induced by Electronic Transitions, DIET V* (Ref. 3), p. 167.
- ⁸A. R. Burns, *Phys. Rev. Lett.* **55**, 525 (1985), *J. Vac. Sci. Technol. A* **4**, 1499 (1986); A. R. Burns, E. B. Stechel, and D. R. Jennison, *Phys. Rev. Lett.* **58**, 250 (1987).
- ⁹P. Feulner, W. Riedel, and D. Menzel, *Phys. Rev. Lett.* **50**, 986 (1983); P. Feulner, D. Menzel, H. Y. Kreuzer, and Z. W. Gortel, *ibid.* **53**, 671 (1984); P. Feulner, R. Treichler, and D. Menzel, *Phys. Rev. B* **24**, 7427 (1981).
- ¹⁰M. Alvey, M. Dresser, and J. T. Yates, Jr., *Phys. Rev. Lett.* **56**, 367 (1986).
- ¹¹F. L. Rook, R. E. Johnson, and W. L. Brown, *Surf. Sci.* **164**, 625 (1985); O. Ellegaard, J. Schou, H. Sørensen, and P. Børgesen, *ibid.* **167**, 474 (1986).
- ¹²D. B. Chrisey, W. L. Brown, and J. W. Boring, *Surf. Sci.* **225**, 130 (1990).
- ¹³W. L. Brown, W. M. Augustyniak, K. J. Marcantonio, E. H. Simmons, J. W. Boring, R. E. Johnson, and C. T. Reimann, *Nucl. Instrum. Methods Phys. Res. Sect. B* **1**, 307 (1984); J. Schou, O. Ellegaard, P. Børgesen, and H. Sørensen, in *Desorption Induced by Electronic Transitions, DIET II*, edited by W. Brenig and D. Menzel (Springer, Berlin, 1985); R. E. Johnson, M. Pospieszalska, and W. L. Brown, *Phys. Rev. B* **44**, 7263 (1991); O. Ellegaard, J. Schou, B. Stenum, H. Sørensen, R. Pedrys, B. Warczak, D. J. Oostra, A. Haring, and A. E. de Vries, *Surf. Sci.* **302**, 371 (1994).
- ¹⁴R. Pedrys, D. J. Oostra, A. Haring, A. E. de Vries, and J. Schou, *Radiat. Eff. Defects Solids* **109**, 130 (1989).
- ¹⁵E. Hudel, E. Steinacker, and P. Feulner, *Surf. Sci.* **273**, 405 (1992).
- ¹⁶K. P. Huber and G. Herzberg, *Constants of Diatomic Molecules* (Van Nostrand Reinhold, New York, 1979); A. Lofthus and P. H. Krupenie, *J. Phys. Chem. Ref. Data* **6**, 113 (1977); S. G. Tilford and J. D. Simmons, *ibid.* **1**, 147 (1972).
- ¹⁷W. Lichten, *J. Chem. Phys.* **26**, 306 (1957); J. Olmsted III, A. S. Newton, and K. Street, Jr., *J. Chem. Phys.* **42**, 2321 (1965);

- R. Clampitt and A. S. Newton, *ibid.* **50**, 1997 (1969); J. M. Ajello, *ibid.* **55**, 3158 (1971); W. L. Borst, *Phys. Rev. A* **5**, 648 (1972); W. L. Borst, W. C. Wells, and E. C. Zipf, *ibid.* **5**, 1744 (1972); J. N. H. Brunt, G. C. King, and F. H. Read, *J. Phys. B* **11**, 173 (1978); D.S. Newman, M. Zubek, and G. C. King, *ibid.* **16**, 2247 (1983); P. Hammond, G. C. King, J. Jureta, and F. H. Read, *ibid.* **20**, 4255 (1987); L. R. LeClair, M. D. Brown, and J. W. McConkey, *Chem. Phys.* **189**, 769 (1994).
- ¹⁸W. L. Borst and E. C. Zipf, *Phys. Rev. A* **3**, 979 (1971).
- ¹⁹R. M. Marsolais, M. Michaud, and L. Sanche, *Phys. Rev. A* **35**, 607 (1987).
- ²⁰D. C. Cartwright, S. Trajmar, A. Chutjian, and W. Williams, *Phys. Rev. A* **16**, 1041 (1977); M. Zubek and G. C. King, *J. Phys. B* **27**, 2613 (1994).
- ²¹A. W. Kam and F. M. Pipkin, *Phys. Rev. A* **43**, 3279 (1991).
- ²²G. J. Schulz, *Rev. Mod. Phys.* **45**, 378 (1973); J. Mazeau, R. I. Hall, G. Joyez, M. Landau, and J. Reinhardt, *J. Phys. B* **6**, 873 (1973).
- ²³R. W. Field, O. Benoist d'Azy, M. Lavollée, R. Lopez-Delgado, and A. Tramer, *J. Chem. Phys.* **78**, 2838 (1983).
- ²⁴S. Cui, R. E. Johnson, and P. T. Cummings, *Phys. Rev. B* **39**, 9580 (1989); W. T. Buller and R. E. Johnson, *ibid.* **43**, 6118 (1991).
- ²⁵J. Heidberg, H. Stein, and E. Riehl, *Phys. Rev. Lett.* **49**, 666 (1982).
- ²⁶T. J. Chuang, *J. Chem. Phys.* **76**, 3828 (1982); T. J. Chuang and H. Seki, *Phys. Rev. Lett.* **49**, 382 (1982).
- ²⁷T. J. Chuang, H. Seki, and I. Hussla, *Surf. Sci.* **158**, 525 (1985); I. Hussla, H. Seki, T. J. Chuang, Z. W. Gortel, H. J. Kreuzer, and P. Piercy, *Phys. Rev. B* **32**, 3489 (1985).
- ²⁸D. Lucas and G. E. Ewing, *Chem. Phys.* **58**, 385 (1981).
- ²⁹H. J. Kreuzer and D. N. Lowy, *Chem. Phys. Lett.* **78**, 50 (1981); Z. W. Gortel, H. J. Kreuzer, P. Piercy, and R. Teshima, *Phys. Rev. B* **27**, 5066 (1983); **28**, 2119 (1983); H. J. Kreuzer and Z. W. Gortel, *ibid.* **29**, 6926 (1984).
- ³⁰F. Dzegilenko, E. Herbst, and T. Uzer, *J. Chem. Phys.* **102**, 2593 (1995), and citations therein; E. Galloway and E. Herbst, *Astron. Astrophys.* **287**, 633 (1994).
- ³¹B. Fain and S. H. Lin, *Chem. Phys. Lett.* **114**, 497 (1985); B. Fain, *ibid.* **118**, 283 (1985).
- ³²M. Michaud and L. Sanche, *Phys. Rev. B* **50**, 4725 (1994).
- ³³G. Bader, G. Perluzzo, L. G. Caron, and L. Sanche, *Phys. Rev. B* **30**, 78 (1984).
- ³⁴A. Mann, P. Cloutier, D. Liu, and L. Sanche, *Phys. Rev. B* **51**, 7200 (1995).
- ³⁵H. A. van Sprang, G. R. Möhlmann, and F. J. de Heer, *Chem. Phys.* **24**, 429 (1977); S. Shadfar, S. R. Lorentz, W. C. Paske, and D. E. Golden, *J. Chem. Phys.* **76**, 5838 (1982).
- ³⁶O. Oehler, D. A. Smith, and K. Dressler, *J. Chem. Phys.* **66**, 2097 (1977).
- ³⁷D. Kuszner and N. Schwentner, *J. Chem. Phys.* **98**, 6965 (1993).